ROLE OF HETEROGENEITIES IN THE CRAZING OF GLASSY POLYMERS

A. S. ARGON
Massachusetts Institute of Technology, Cambridge, Massachusetts 02139, USA

ABSTRACT

Crazing in glassy polymers is strongly influenced by heterogeneities at many levels starting from the dense molecular entanglements that can produce micropores by obstructing localized shear, and going up in scale to different polymer phases, particulate inclusions, patches of oriented polymer produced by shear deformation bands, and finally, surface grooves and scratches which can act as internal or surface stress concentrators to initiate dilational localization to form the crazes. These points are discussed semi-quantitatively in the light of some recent experiments on crazing.

1. INTRODUCTION

The mechanical properties and behaviour of polymers are influenced strongly by heterogeneities. Such heterogeneities may either occur accidentally or could be incorporated deliberately. Their effects could be either beneficial or deleterious. Such opposite effects are often produced by one and the same heterogeneity: it is essential therefore, that their role be properly understood. Heterogeneities can produce some non-synergistic effects which can be accounted for merely in the proportion of the volume they occupy, independent of size and distribution of the heterogeneity. Elastic moduli, and some transport properties such as permeability, etc., are of this type. In many other instances, however, heterogeneities catalyse effects which depend also on their size, shape and distribution. Much of mechanical behaviour, especially as it relates to ultimate performance, is of this latter type. We will concern ourselves in this contribution primarily with some of the more important synergistic effects of heterogeneities on ultimate mechanical behaviour of polymers.

2. TYPES OF HETEROGENEITIES IN POLYMERS

The word *homogeneous* refers to a uniform constitution of matter, which in polymers can only be considered as an idealization. Leaving out differences in molecular weight distribution and differences in tacticity, and concentrating only on states of aggregation on a scale much larger than molecular diameters or size of monomer repeat units, it would be difficult to find any solid polymer which is truly homogeneous. A widely appreciated form of heterogeneity in single-component polymers is their degree of crystallinity and the ways it

can be affected by thermomechanical treatment[1–4]. A more elusive and controversial form of heterogeneity is the nodules which have been reported to occur on the scale of tens of ångströms in glassy polymers, based on direct observation in thin films[5–7] and on indirect experiments on reactivity[8]. Their presence has, however, been doubted on thermodynamical grounds[9], and specially designed neutron diffraction experiments[10] have given negative results. By far the technologically most important heterogeneities, however, relate to multi-phase structures resulting alternatively: from the blending of generally immiscible components of polymers; or from phase separation of block and graft copolymers. The shapes and dispersion of such heterogeneous phases can be controlled to a wide degree by control of composition affecting the nature of the phase separation[11–13], and by thermomechanical treatment[14]. In the instances when the heterogeneities consist of an elastomeric phase in a normally brittle glassy polymer, they can impart very attractive toughness by initiating modes of inhomogeneous deformation in the form of localized bands of shear or dilatation (crazing). These tend to interact with each other to nucleate more of the same and give rise to large amounts of energy absorbing inelastic deformation. In addition to such natural heterogeneities, a whole range of artificial heterogeneities in the form of hard spherical particles or short fibres have been used to approximate to the behaviour of the natural heterogeneities[15]. We distinguish these latter applications from the very wide range of applications of polymers as a matrix material in composites where the main advantage is derived from the properties of the reinforcing phase of fibres or plates, and where polymers act merely as a binder and as a traction transmitting agency[16, 17]. The subject of composites has been extensively investigated and will not be part of our concern. The interested reader can consult many excellent treatises on this subject, such as, e.g., that of Kelly[18].

Finally, however, two other types of heterogeneity must be considered which have profound effects on ultimate behaviour: accidental particulate inclusions and surface scratches, which can both nucleate inhomogeneous deformation and cause fracture.

In this contribution we will be primarily concerned with the restricted area of heterogeneities in glassy polymers which synergistically affect their ultimate behaviour, and with the mechanisms of inelastic deformation which such heterogeneities initiate. We will not be concerned with the role of heterogeneities in non-synergistic behaviour such as elastic and viscoelastic properties. The interested reader is referred to the treatments of these subjects in the recent literature[19–22].

3. PROCESSES OF INELASTIC DEFORMATION IN GLASSY POLYMERS

Below the glass transition temperature the strain rate response of glassy polymers to increasing shear stress is first linear but then becomes increasingly non-linear. For stresses significantly less than 0.01 of the shear modulus the polymer shows a linearly viscoelastic response. With increasing stress the response becomes non-linearly viscoelastic above a stress-to-modulus ratio of 0.01, and finally plastic when the ratio exceeds about 0.05. This ratio where

plasticity sets in increases with decreasing temperature and reaches an asymptotic value of around 0.1–0.12 at 0K. For a given stress the strain rate, whether viscoelastic or plastic, has a temperature dependence which is of a nearly Arrhenius form. In addition, the plastic flow stress for a given strain rate increases somewhat with increasing pressure. This is the dilatation-free distortional behaviour of glassy polymers the mechanisms of which have recently been discussed by Argon[23]. It obeys a pressure dependent Mises yield criterion, and may in some cases localize into intense shear deformation bands, when a molecular strain softening process exists. Here we will not be overly concerned with the distortional plastic behaviour of glassy polymers beyond stating that when shear deformation localization occurs, the resulting shear bands incorporate highly aligned polymeric material which can then act as a new form of planar heterogeneity.

Of more interest to us will be the *crazing* process (dilatational plasticity) in polymers, which occurs in all glassy polymers below the level of distortional yielding when the applied stress has a negative pressure (dilatational) component. Crazes are zones of cavitational deformation occurring in initially unoriented polymers, always normal to the maximum principal tensile stress. They are often precursors of cracks. The morphology of crazes and their phenomenology have recently been reviewed extensively by both Rabinowitz and Beardmore[24] and by Kambour[25]. The uninitiated reader is strongly advised to refer to these papers. A physical mechanism for formation of crazes has been proposed by Argon[26]. Since this mechanism will be of central importance in our discussion on the ultimate behaviour of glassy polymers, we will give a brief review of this mechanism and then apply it to the case of nucleation of crazes from heterogeneities.

4. MECHANISM OF CRAZE NUCLEATION IN GLASSY POLYMERS

The kinetics of nucleation of crazes and the complex stress condition which describes their isochronous formation suggest that crazing consists of three relatively distinct stages which are, in order: thermally activated production of stable micro-porosity under stress; formation of a craze nucleus by plastic expansion of holes in a small region while elastically unloading the surroundings; and extension of the craze nucleus into a planar 'yield' zone.

Apart from the small amount of free volume which every polymer has at a molecular level below its glass transition temperature, we assume that the starting polymer is continuous and free of holes. In Stage I, under an applied stress, below that of general yield, the polymer undergoes a stable, thermally activated cavitation in regions of stress concentration which produces holes of ~ 100 Å size. This is the process that has been studied in detail by Zhurkov and co-workers[27, 28] by low-angle x-ray scattering and e.s.r., and has recently been observed by Baer and Wellinghoff[29] directly in thin polystyrene films stretched on Mylar films and subsequently examined in the electron microscope where the holes have been revealed by precipitation of iodine. Zhurkov's observation on the stress dependence of the cavity generation rate is of the form

$$\frac{\mathrm{d}\beta}{\mathrm{d}t} = \dot{\beta}_0 \exp\left(-\frac{U - \sigma_N v}{kT}\right) \tag{1}$$

where β is the porosity, $\dot{\beta}_0$ is a constant pre-exponential term, U is the extrapolated activation energy at zero stress, σ_N is the applied tensile stress and v is an activation volume. Both U and v are obtained by analysing experimental data.

For several reasons which will become clear later we find it necessary to derive a more specific expression for porosity formation.

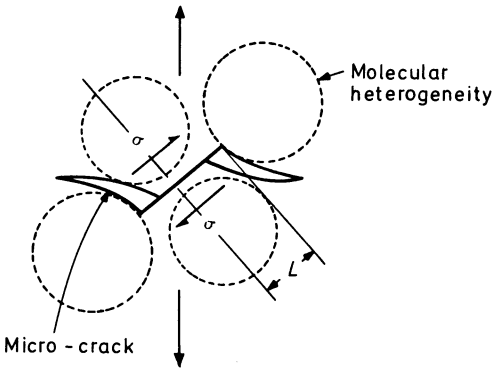

Figure 1. Formation of micro-cracks by arrest of micro-shear bands

In *Figure 1* we consider a region of stress concentration, either at the root of a surface groove or near the interface of an internal heterogeneity where thermally activated plastic flow is possible under the locally amplified *shear* stress σ. If a molecular strain softening process exists at least over a very local scale, it becomes possible to treat the initiation and small-scale localization of the plastic shear process as a one-step nucleation event in the form of a shear patch of radius R and of vanishing thickness which, as discussed by Thierry, Oxborough and Bowden[30], is the energetically most advantageous form for local stress relaxation. Based on the analogue of dislocation loop formation, the free enthalpy ΔG for activation for the shear patch under an applied shear stress σ could then be written as a first approximation as

$$\Delta G = \Delta F - \Delta W = 2\pi R\mathscr{E} - \pi R^2\sigma\varphi \tag{2}$$

where

$$\mathscr{E} \simeq 0.15\,\mu\varphi^2 \tag{3}$$

is the line energy stored around the periphery of the sheared patch per unit length, μ is the shear modulus and φ is the relative displacement across the sheared region, which must be of the order of the molecular diameter †.

† The magnitude 0.15 for the coefficient of the line energy is a good estimate which incorporates interactions of all segments of the circumference of the patch and is chosen for a ratio of patch radius to sheared displacement, (R/φ), of about 4–5. The actual computation of the saddle point in the free enthalpy is far more complicated than the simple asymptotic form given here. It is strongly model sensitive and depends on the particular form of the intermolecular shear resistance where that resistance reaches its maximum value.

The saddle point in the free enthalpy is obtained from

$$(\partial \Delta G/\partial R)_{\varphi,\sigma} = 0 \tag{4}$$

which gives

$$R^* = \mathscr{E}/\sigma\varphi \tag{5}$$

and

$$\Delta G^* = \pi(\mathscr{E}^2/\sigma\varphi) = (0.15)^2\pi(\mu/\sigma)(\mu\varphi^3) \tag{6}$$

Considering that glassy polymers have shear moduli $\mu \simeq 10^{10}$ dyn/cm^2 and average molecular diameters $\varphi = 3 \times 10^{-8}$, the activation free enthalpy for a shear stress $\sigma \simeq (\mu/25)$ would give $R^* \simeq 4\varphi$ and $\Delta G^* \simeq 0.3$ eV—values which are quite reasonable for a room temperature process. Once the patch reaches its critical configuration, the shear deformation can continue to spread out in the plane of the patch at a falling stress, without being dispersed[23]. The growth of the patch could be arrested at molecular heterogeneities with higher shear resistance. These heterogeneities may, e.g., be dense molecular entanglements. It is of no great concern to us here whether or not such heterogeneities represent regions of higher crystallinity. We require from them only a higher than average plastic shear resistance capable of stopping the patch of micro-shear. At the ends where the patch is blocked local stress concentrations will arise which produce a normal stress σ_N of the order of[31]

$$\sigma_N \simeq \sigma(L/\varphi)^{\frac{1}{2}} \tag{7}$$

Since the ratio L/φ of the heterogeneity spacing to relative displacement is likely to be of order ten, local tensile stresses in excess of three times the shear resistance can be produced which could well equal the cohesive strength of the polymer to open up micro-cracks as shown in *Figure 1*. The only additional requirement for such cracks is that enough energy be stored in the local region to provide for the surface free energy of the micro-cracks, i.e.

$$\frac{1}{2E}\left(\sigma\sqrt{\frac{L}{\varphi}}\right)^2 \pi\left(\frac{L}{2}\right)^3 \gtrsim 2\left(\frac{\pi}{2}\right)\left(\frac{L}{2}\right)^2 \alpha \tag{8}$$

$$\frac{\sigma^2 L^2}{4\varphi E} \gtrsim \alpha \tag{9}$$

where α is the specific surface energy of the polymer and E is its Young's modulus. The condition given in equation (9) is in a realizable range. It is interesting to note that the formation of micro-cracks just discussed could occur entirely by separating molecules against their intermolecular attractions without necessarily severing any primary bonds. Recent e.s.r. measurements by Nielsen[32] in which no detectable free radical generation was observed during crazing lends support to this possibility. We observe, furthermore, that as long as inequality (9) is satisfied, pore nucleation is all but accomplished when the energy barrier for the shear patch has been overcome, without requiring overcoming any additional energy barrier.

On the basis of the above mechanism, we expect that the initial development of micro-porosity with time will have a form of

$$\beta(t) = \dot{\beta}_0 t \exp(-\Delta G^*(s)/kT) \tag{10}$$

where the activation free enthalpy is given by equation (6) and where we have already generalized the result from an applied shear stress to the local deviatoric shear stress s (the root mean square shear stress in multi-axial stressing) in the vicinity of the surface or interface stress concentration, given by the well-known expression involving the principal stresses:

$$s = [(1/6)\{(\sigma_1 - \sigma_2)^2 + (\sigma_2 - \sigma_3)^2 + (\sigma_3 - \sigma_1)^2\}]^{\frac{1}{2}} \tag{11}$$

It is well to emphasize here that in our model pores form as a result of local inhomogeneous plastic deformation at stress levels a factor of two or three below those of general yield; hence, stress concentrations play a fundamental role.

When the local porosity reaches a critical magnitude, depending upon the local stress state, a condition of rapid plastic expansion of holes becomes possible in an equiaxed region at the expense of elastically unloading the surroundings. This is Stage II, in which visible craze nuclei form during a comparatively short time governed by the rate of plastic expansion of the holes.

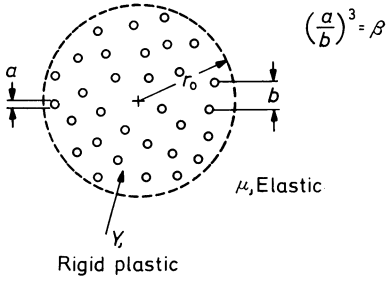

Figure 2. Rigid plastic region about to undergo cavitation under the action of a negative pressure applied by elastic surroundings

As shown in *Figure 2*, we consider a porous, roughly spherical region of radius r_0 in which the material is idealized as rigid with a tensile plastic resistance Y which is strain rate, temperature and pressure dependent, and equal to $\sqrt{3}\tau(p, T, \dot{\gamma})$, where τ is the distortional plastic resistance in shear discussed above†. Outside the porosity inhomogeneity the material is idealized as perfectly elastic. Rice and Tracy[33], who have analysed the fully plastic growth of initially spherical holes under arbitrary states of stress, have concluded that the net growth of a hole in a rigid plastic material depends substantially only on the negative pressure, with the shear stresses contributing to this growth only in a secondary manner. The effect of the deviatoric shear stress, however, cannot be entirely neglected. When it is very large and

† The plastic resistance of a glassy polymer increases with large extension ratios. Incorporation of such hardening into the equations, however, produces no significant change in the condition for pore expansion[26].

near yield, only relatively small amounts of negative pressure are sufficient to expand holes, albeit rather slowly. McClintock and Stowers[34] have recently analysed the growth of holes under combined negative pressure and deviatoric shear stress. Their results, shown in *Figure 3*, demonstrate that when the porosity is small (~ 0.01), only deviatoric shear stresses greater than 0.8τ begin to play a significant role in reducing the required negative pressure for hole expansion. On the basis of these results, we can now write the stress condition for expansion of pores as (see reference 26 for further details):

$$p = (2Y/3) \ln (1/\beta) [Q(s/Y)] \tag{12}$$

where p stands for *negative* pressure and $Q(s/Y)$ is the normalized locus for pore expansion given in *Figure 3*. The value of Q is near unity for $s/Y < 0.8/\sqrt{3}$,

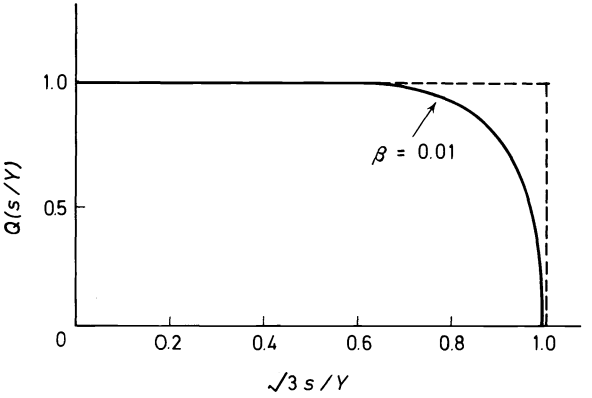

Figure 3. Locus of pore expansion under a combination of negative pressure and deviatoric shear stress: solid curve after McClintock and Stowers[34]; dotted box, asymptotic idealization

where its effect can be neglected. As a first approximation we will replace Q by the box-shaped locus shown in *Figure 3*, which amounts to computing asymptotic and non-interacting behaviour for the s- and p-components of the stress tensor. This will give satisfactory results except for the discussion of asymptotic craze densities, where Q and its specific dependence on s/Y are of crucial importance.

The negative pressure given in equation (12) is not a sufficient condition for the rapid extension of pores in the region of porosity inhomogeneity. Since this negative pressure for the continued plastic expansion of the holes is applied over the boundary of the region by the elastic surroundings which would be unloaded by the expansion of holes in the region of radius r_0, we must require also that the rate of decrease of boundary traction due to external elastic unloading be less rapid than the allowable decrease of the negative pressure with increasing porosity, i.e.

$$|d\sigma_{rr}/dr| < |dp/dr| \tag{13}$$

The left-hand side of inequality (12) is the radial stiffness of a spherical hole in an elastic continuum and is given by

$$d\sigma_{rr}/dr = -4\mu/r_0$$

where r_0 is the initial radius of the inhomogeneity. The right-hand side of inequality (13) is obtainable from equation (12) and the condition of compatibility as

$$(\mathrm{d}p/\mathrm{d}r) = -(2Y/\beta_i r_0)(1 - \beta_i) \tag{14}$$

for the start of the process where $\beta = \beta_i$, where, as stated above, Q was set equal to unity. The condition given by equation (13) prescribes a critical initial porosity, β_{crit}, which cannot be exceeded if the Stage II process of craze nucleus formation by an elastic–plastic unloading is to occur. This critical initial porosity is

$$\beta_{crit} = 1/(1 + 2\mu/Y) \tag{15}$$

Hence, the two conditions for craze nucleus formation in Stage II can be stated as

$$p = (2Y/3)\ln(1/\beta) \tag{16a}$$

$$\beta_i < 1/(1 + 2\mu/Y) \tag{16b}$$

The development of Stage II is sketched in *Figure 4*. The curved line gives the asymptotic negative pressure (for $Q = 1$). For a local level of applied

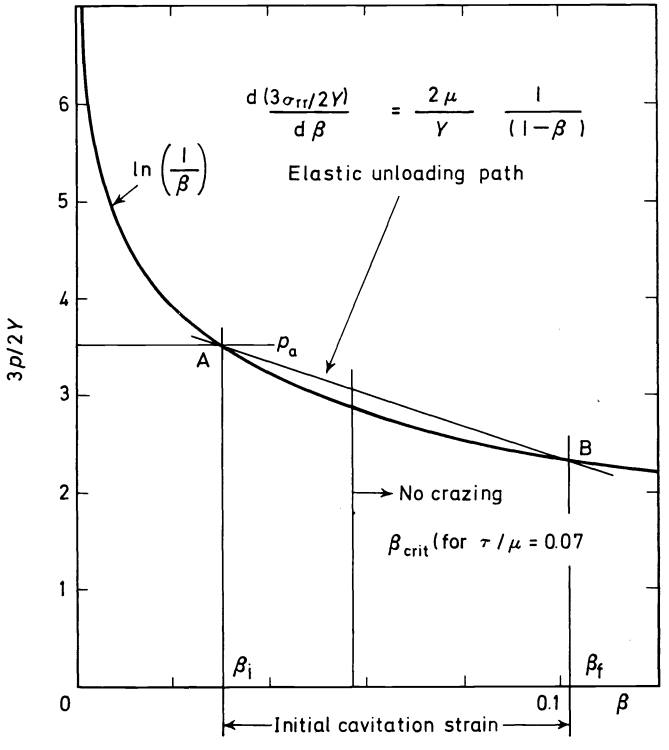

Figure 4. Process history for elastic–plastic cavitation (from reference 26, courtesy of Marcel Dekker Inc.)

negative pressure p_a, the process of cavitational localization cannot start before the porosity reaches β_i by the micro-pore formation process. When β finally reaches this magnitude, provided $\beta_i < \beta_{crit}$, the local radial stress will unload from A along the slanted line to B, producing an initial volumetric crazing strain of $\beta_f - \beta_i$ in the interior of the spherical region. *Figure 4* is drawn to scale and the construction is for a ratio of $Y/\mu = 0.12$, ($\tau/\mu = 0.07$), which represents the conditions for polystyrene at room temperature for which $\beta_{crit} = 0.057$. If the local negative pressure at a root of a surface scratch is such that $3p_a/2Y$ is about 3.5 (a rather high ratio), then the cavity expansion process will begin at an initial local porosity of 0.03 and the initial volumetric cavitation strain will be only 0.072. Thus the normally reported large volumetric strains for mature crazes must develop after the nucleation.

We note that as temperature increases, Y/μ and β_{crit} decrease. Above a temperature where $\beta_{crit} < \beta_i$ for the given applied negative pressure p_a, craze nucleation is no longer possible, since the rate of elastic unloading of the surroundings exceeds the allowable rate of drop of negative pressure for hole expansion. Naturally the polymer could still go on cavitating in a quasi-homogeneous manner. Combining equations (10) and (16a) gives the general conditions for craze nucleation as

$$3p/2Y = -\ln \dot{\beta}_0 t + \Delta G^*(s)/kT \tag{17}$$

We take this as the local condition for craze nucleation, where p and s stand for the local concentrated stresses. This is then the criterion which must be applied for craze nucleation at interfaces of heterogeneities, etc., where, of course, the local stresses may first have to be found by the solution of a boundary value problem. We now proceed to compute the external stress conditions for craze nucleation on a sample with a collection of average surface scratches.

5. EFFECT OF SURFACE STRESS CONCENTRATIONS ON CRAZE NUCLEATION

In experiments under biaxial stress ($\sigma_3 = 0$) Sternstein and Ongchin[35] have found a phenomenological, isochronous (10 min) crazing criterion for glassy polymers which they have stated as

$$|\sigma_1 - \sigma_2| = -A(T) + B(T)/(\sigma_1 + \sigma_2) \tag{18}$$

We will now show that if the local craze nucleation criterion derived in the preceding section is applied to a polymer with surface stress concentrations, Sternstein and Ongchin's equation is obtained.

To begin, we assume that, unless extreme precautions are taken, the surfaces of all polymers have a large collection of accidentally produced scratches and grooves which would be randomly oriented relative to applied biaxial stresses σ_1 and σ_2. As shown in *Figure 5*, let us consider a typical surface scratch at an angle θ relative to the principal stress σ_1. Thus, in the natural coordinates of the scratch it is subjected to stresses σ_{11}, σ_{22} and σ_{12}, of which σ_{22} and σ_{12} will be concentrated, while σ_{11} will not produce a significant concentration. There are, of course, scratches at all angles and of a variety of depths. For the time being, we consider them all of constant

depth producing the same stress concentration under similar orientations with the applied principal stresses. Since the craze nucleation criterion involves both a deviatoric shear stress and a negative pressure, it is not necessary that the scratches which nucleate crazes in the shortest time be oriented normal to the maximum principal tensile stress, even though this is the direction across which crazes tend to *grow*. The scratches which are most effective in craze nucleation are those which minimize the crazing time in

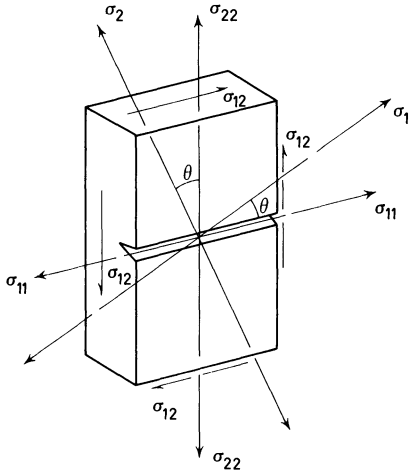

Figure 5. Surface groove under the application of a biaxial state of stress

equation (17). Hence, we proceed by obtaining the deviatoric shear stress and negative pressure for an arbitrary scratch at an angle θ, substitute these stresses in equation (17) and minimize the craze nucleation time.

The stresses σ_{11}, σ_{22}, σ_{12} referred to the axes of the scratch are

$$\sigma_{22} = \tfrac{1}{2}(\sigma_1 + \sigma_2) + \tfrac{1}{2}(\sigma_2 - \sigma_1)\cos 2\theta \tag{19a}$$

$$\sigma_{11} = \tfrac{1}{2}(\sigma_1 + \sigma_2) - \tfrac{1}{2}(\sigma_2 - \sigma_1)\cos 2\theta \tag{19b}$$

$$\sigma_{12} = \tfrac{1}{2}(\sigma_2 - \sigma_1)\sin 2\theta \tag{19c}$$

where $\sigma_2 < \sigma_1$ was assumed. Considering an asymptotic behaviour for only deep scratches, and that the material will be at yield at the grooves of the scratches, we can write the concentrated stresses, σ'_{22}, σ'_{11}, σ'_{12}, as:

$$\sigma'_{22}/Y = f\xi + f\eta\cos 2\theta \tag{20a}$$

$$\sigma'_{11}/Y = \tfrac{1}{2}f\xi + \tfrac{1}{2}f\eta\cos 2\theta \tag{20b}$$

$$\sigma'_{12}/Y = f\eta\sin 2\theta \tag{20c}$$

where f stands for the asymptotic stress concentration factor for deep scratches, which is assumed to be equal for plane strain and anti-plane strain, where the significant stress σ'_{11} is considered to arise primarily from plane strain

conditions, and where in anticipation of later ease the following normalizations were introduced: $\xi = (\sigma_2 + \sigma_1)/2Y$ and $\eta = (\sigma_2 - \sigma_1)/2Y$. The local normalized deviatoric shear stress and negative pressure can now be obtained by substitution of equations (20a)–(20c) into

$$s^2 = \tfrac{1}{6}[(\sigma'_{11} - \sigma'_{22})^2 + (\sigma'_{22} - \sigma'_{33})^2 + (\sigma'_{33} - \sigma'_{11})^2] + \sigma'^2_{12} \tag{21a}$$

$$p = \tfrac{1}{3}[\sigma'_{11} + \sigma'_{22} + \sigma'_{33}] \tag{21b}$$

where $\sigma'_{33} = 0$ is assumed. This gives

$$s^2 = \tfrac{1}{4}f^2Y^2(\xi + \eta\cos 2\theta)^2 + f^2Y^2(\eta \sin 2\theta)^2 \tag{22a}$$

$$p = \tfrac{1}{2}fY(\xi + \eta\cos 2\theta) \tag{22b}$$

We require that upon substitution of the contents of equations (22a) and (22b) into equation (17), the crazing time in the latter be minimized with θ, i.e.

$$\frac{\partial \ln \dot{\beta}_0 t}{\partial\theta} = \frac{\partial}{\partial\theta}\left(\frac{A/Y}{s/Y}\right) - \frac{\partial}{\partial\theta}\left(\frac{\frac{3}{2}(p/Y)}{Q(s/Y)}\right) = 0 \tag{23}$$

where $A = \pi\mathscr{E}^2/\varphi kT$ is the coefficient of the reciprocal deviatoric shear stress in the exponential of equation (10) giving the time law of porosity development. But

$$\frac{\partial \ln \dot{\beta}_0 t}{\partial\theta} = \left(\frac{\partial \ln \dot{\beta}_0 t}{\partial(s/Y)}\right)_\xi \frac{\partial(s/Y)}{\partial\theta} + \left(\frac{\partial \ln \dot{\beta}_0 t}{\partial(p/Y)}\right)_\eta \frac{\partial(p/Y)}{\partial\theta} \tag{24}$$

Computation of the various partial derivatives gives for the condition of the minimum

$$\left[\left(-\frac{(A/Y)}{2(s/Y)^3} + \frac{(\frac{3}{2})(p/Y)}{2(s/Y)Q^2}\frac{\partial Q}{\partial(s/Y)}\right) f^2(3\eta^2\cos 2\theta - \eta\xi) + \frac{3}{2}\frac{f\eta}{Q}\right]\sin 2\theta = 0 \tag{25}$$

The first condition for an extremum in the time for craze nucleation is

$$\sin 2\theta = 0 \tag{26}$$

The second condition is obtained upon inspection of equation (25). In this equation the first two terms which are always negative dominate in absolute value the last term by an order of magnitude or more; hence, a second condition for an extremum is

$$\cos 2\theta = \xi/3\eta \tag{27}$$

Substitution of conditions (26) and (27) into equations (22a) and (22b) and these into equation (17) gives in abbreviated notation two crazing conditions:

$$(1/f)\ln \dot{\beta}_0 t = (A/Yf^2)/\tfrac{1}{2}(\xi + \eta) - (\tfrac{3}{2})(\tfrac{1}{2})(\xi + \eta) \tag{28a}$$

$$(1/f)\ln \dot{\beta}_0 t = (A/Yf^2)/[\tfrac{1}{3}\xi^2 + \eta^2]^{\frac{1}{2}} - \xi \tag{28b}$$

Of these two conditions, the second one nearly always governs, as will become clear further below. We abbreviate further by calling $\alpha = A/Yf^2$ and $\delta = (\ln \dot{\beta}_0 t)/f$. As will be demonstrated below, the value of the average surface stress concentration factor is around 3.5, which together with the previously

introduced magnitudes for the activation free enthalpy gives $\alpha \approx 0.55$. The value for δ is less readily obtainable from fundamental considerations. To obtain a reasonable fit to the phenomenological stress condition of Sternstein and Ongchin[35] we pick $\delta = \frac{1}{2}\alpha$. This would give for the pre-exponential factor $\dot{\beta}_0 = 2.6 \times 10^{-2}\ s^{-1}$. The isochronous biaxial locus for craze initiation computed from equation (28b) is shown in *Figure 6* for $\alpha = 0.55$ and $\delta = \frac{1}{2}\alpha$,

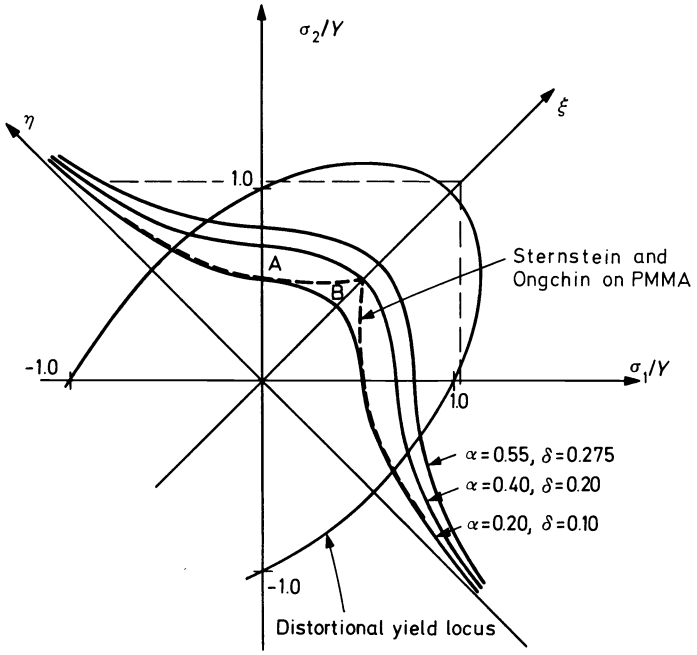

Figure 6. Biaxial locus for craze initiation: solid curves, computed on basis of equation (28b); broken straight line sections, computed on basis of equation (28a); broken cuspy curve, experimental observation of Sternstein and Ongchin[35]. The elliptical distortional yield locus is given for comparison

together with the locus for distortional yielding for comparison. On the other hand, the condition given by equation (28a) for the same coefficients α and δ is given by the dotted straight lines in *Figure 6*. Clearly, since this condition requires considerably larger stresses than those given by equation (28b), it will not govern in the range of interest. If the surface contains more severe stress concentrations or if the activation free enthalpy given in equation (6) should have been overestimated, the isochronous craze nucleation loci would lie below the upper curve shown in *Figure 6*. Two other curves computed for coefficients $\alpha = 0.4$ and $\alpha = 0.2$ are also plotted in *Figure 6*. The one for $\alpha = 0.2$ corresponds more closely to the phenomenological curve presented by Sternstein and Ongchin[35] for PMMA at room temperature which is also reproduced in *Figure 6*. The craze initiation locus computed from our theoretical model produces a good fit to the experimental locus obtained by Sternstein and Ongchin everywhere except in the region of nearly equal

biaxial stress, where it lies considerably below the experimental locus. This could have two reasons. First, our theory as described above considers stress concentrations only in an asymptotic form as if they were of singular nature. This could therefore artificially suppress the locus in certain regions. Second, the experimentally obtained craze condition of Sternstein and Ongchin is most likely not purely for craze nucleation alone but must involve some craze growth as well. Therefore, if the real isochronous craze nucleation condition were as given by equation (28b), in the equal biaxial stress region shown by point B in *Figure 6*, crazes would nucleate as rapidly as those given by the stress state at point A, but would grow considerably less rapidly than those at point A. Hence, in experimental observations there would be a tendency to overestimate the crazing condition in the case of equal biaxial stress.

Finally, it is worth pointing out here that the distortional yield locus shown in *Figure 6* is truly a surface of a plastic potential for which an associated flow rule will hold (see reference 23 for the correct interpretation of the associated flow rule for a pressure dependent yield condition). The craze locus shown in *Figure 6*, on the other hand, is only a 'plastic potential' for the minute inelastic strains associated with the craze nucleation. Once crazes have nucleated in an initially isotropic polymer, they grow in a direction perpendicular to the maximum principal tensile stress regardless of the magnitude and sign of the other principal stresses (so long as they do not produce general yielding together with the maximum principal tensile stress). Thus the inelastic strain increments resulting from craze growth will not form a set that is normal to the locus of craze initiation. A most important corollary to this observation is that the craze initiation locus does not outline the regions in stress space for craze-free operation. Experiments[36] show that pre-existing crazes grow in response to a tensile stress acting across the plane of the craze, when such a stress exceeds a certain value, and presumably independent of the other principal stresses so long as they are algebraically smaller and do not produce general yield. This important point, however, has not been fully substantiated.

The stress conditions and the actual mechanisms for the growth of crazes from nuclei formed by the process discussed above are not yet completely understood. Initial attempts in modelling the growth of crazes as a repeated process of craze matter production ahead of the craze has shown that this is not likely to happen because of the insufficiency of the levels of deviatoric shear stress and negative pressure ahead of the craze. Instead, craze matter extension both longitudinally and transversely appears to be by the repeated convolution of the polymer–air interface in a manner identical with that observed in the well-known instability of a concave air–liquid meniscus displaced in the direction of the liquid. The details of these findings will be reported in greater detail elsewhere[37].

6. EXPERIMENTAL OBSERVATIONS ON THE EFFECT OF SURFACE STRESS CONCENTRATIONS

Nucleation of crazes from spherical particles

Wang, Matsuo and Kwei[38] have performed experiments on craze initiation from both spherical rubber and steel inclusions in a polystyrene matrix

subjected to uniaxial tension. They found that the position of craze formation occurs along the equator on rubber particles and that this is predicted by a great variety of craze criteria. On the other hand, in the case of spherical steel inclusions crazes appear at an angle of 37° from the point on the sphere immediately under the tensile axis. Among all crazing criteria studied by Wang, Matsuo and Kwei, this is predicted only by a critical tensile strain criterion, and is, e.g., not in agreement with the generalization of the crazing criterion of Sternstein and Ongchin[35]. It was pointed out by several authors[26, 39], however, that Sternstein and Ongchin's interpretation of their so-called stress bias criterion is at best ambiguous. In contrast, the local crazing criterion given in equation (17) has no ambiguity. When it is applied to the findings of Wang, Matsuo and Kwei, it gives as good an agreement as the critical tensile strain criterion.

The local deviatoric shear stress and negative pressure can be given in terms of the distortion energy density W_D and the elastic dilational strain Δ used by these authors as

$$s = (2\mu W_D)^{\frac{1}{2}} = T[\overline{W}_D/(1 + \nu)]^{\frac{1}{2}} \tag{29}$$

$$p = p_0\Delta/\Delta_0 = \tfrac{1}{3}T(\Delta/\Delta_0) \tag{30}$$

where $\overline{W}_D = 2\mu(1 + \nu)W_D/T^2$ is a normalized distortion energy density, Δ_0 and p_0 are the dilational strain and negative pressure far away from the particle and T is the applied tensile stress at which craze initiation at the particle interphase was observed. Substitution of s and p into equation (17) gives

$$\ln \dot{\beta}_0 t = \frac{(A/Y)}{f(T/Y)\{\overline{W}_D(\theta)/(1 + \nu)\}^{\frac{1}{2}}} - \tfrac{3}{2}f\left(\frac{T}{3Y}\right)\left(\frac{\Delta(\theta)}{\Delta_0}\right) \tag{31}$$

where an allowance is made for small stress concentrations f on the interface between the polymer and the spherical steel inclusion. Dividing by f gives

$$\frac{\ln \dot{\beta}_0 t}{f} = \delta = \frac{\alpha}{(T/Y)\{\overline{W}_D(\theta)/(1 + \nu)^{\frac{1}{2}}} - \frac{1}{2}\left(\frac{T}{Y}\right)\left(\frac{\Delta(\theta)}{\Delta_0}\right) \tag{32}$$

The crazes will occur predominantly in the location θ where the function δ expressing the craze initiation time is minimized. *Figure 7* shows the change in the craze initiation time δ as a function of angular position θ for the two values of α used in *Figure 6*, by making use of the angle dependent plots of $\overline{W}_D$ and Δ/Δ_0 given by Wang, Matsuo and Kwei. Clearly, the case for $\alpha = 0.4$ gives excellent agreement with their observations. In the computations of the curves given in *Figure 7* a yield stress $Y = 5700$ lb/in^2 was used by taking the Young's modulus of 1.27×10^5 lb/in^2 given by the authors and by taking the ratio τ/μ of the yield stress in shear to the shear modulus as 0.045 at room temperature, for polystyrene, as given by Argon[40]. The external stress T at which crazes initiated at the interface was taken as 2850 lb/in^2, as given by the authors.

The results in *Figure 7* show that at the minima the ratio of $\alpha/\delta = 2$ which was assumed in *Figure 6* is not preserved. This must be due in part to the

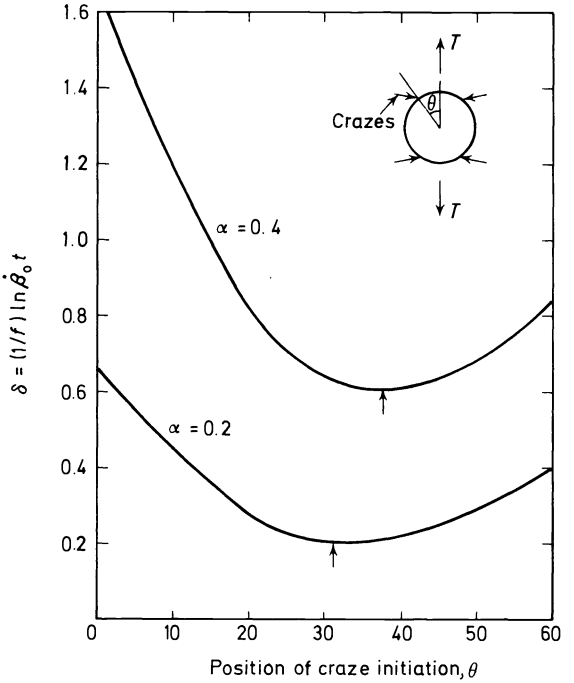

Figure 7. Minimization of craze initiation time as a function of position on surface of rigid inclusion, based on computations of Wang, Matsuo and Kwei[38]

inhomogeneous stress field around the spherical particle which is incorporated in the computations of $\overline{W}_D$ and Δ/Δ_0, but also reflects that a fundamental understanding for the magnitude of the pre-exponential factor $\dot{\beta}_0$ in equation (17) is lacking.

Nucleation of crazes from surface imperfections

In a study of the kinetics of the nucleation of crazes from surfaces subjected to states of stress with different combinations of deviatoric shear, and negative pressure, the details of which will be reported elsewhere[41], it became clear that reproducibility of results is strongly affected by the reproducibility of the surface roughness. As a first step in assuring reproducibility, surfaces of carefully machined tubular specimens were given the highest degree possible of metallographic polish with alumina powders of decreasing sizes down to 0.1 μm until the surfaces became optically featureless and impossible to focus on with a light microscope. The initiation of crazes on such surfaces showed very large scatter. In some instances no crazes could be obtained at all at stress levels under which the same polymer having no special surface preparation was known to show extensive crazing. The stress could be increased on such specimens to values about halfway between the normal craze initiation stress and the macro-yield stress before fracture initiated from an internal particulate flaw, or from the inner surface of the specimen

which could not be as perfectly polished. To make the experiments reproducible, a standard surface roughness was produced by touching the highly polished surfaces with a wet velvet polishing cloth carrying 4 μm size SiC particles for 10 s. A magnified trace of an interference contour obtained with an interference microscope of a typical surface subjected to this roughening treatment is shown in *Figure 8*.

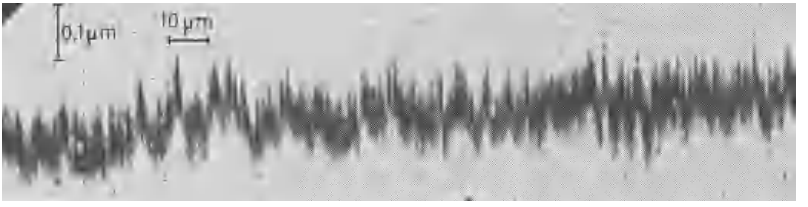

Figure 8. Interference trace, showing roughness of surface on polystyrene specimens used in craze initiation studies

If these grooves are considered to be of elliptical cross-section with a stress concentration factor

$$f = 1 + 2(a/b) \tag{33}$$

where a is the depth of the groove and b its opening at the surface, then the trace in *Figure 8* gives directly the surface density distribution of stress concentrations if b is relatively constant. This distribution is plotted in *Figure 9* to within a constant adjustable multiplier. This multiplier, which is of order unity, results from the fact that the grooves along the circumference of the specimen are not of constant depth but have a secondary wavelength λ resulting from the rolling action of the SiC particles. The amplitude of this secondary roughness is not readily determinable and is taken into account as a constant factor shifting the distribution in *Figure 9* to a somewhat higher value, already incorporated into it as a result of the application to be discussed below.

A set of direct photographic recordings of the development of craze nuclei as a function of time on surfaces of such specimens subjected to a combination of constant axial tension and torsion to produce different combinations of applied deviatoric shear stress s_0 and negative pressure p_0 is given by the experimental points in *Figure 10*. These results show that the density of crazes increases as a function of time under a constant state of stress, and that for a constant applied negative pressure p_0 the curves not only are shifted to shorter times with increasing deviatoric shear stresses but also reach increasing asymptotic craze densities. The shapes of the curves are a direct result of the density distribution of surface stress concentrations. Crazes initiate earlier from sites of large stress concentration, while sites with lower stress concentration require longer time. When the deviatoric shear stress is increased, all processes occur faster and the curves are shifted towards shorter time. The increase in the asymptotic densities of crazes on surfaces with nearly identical

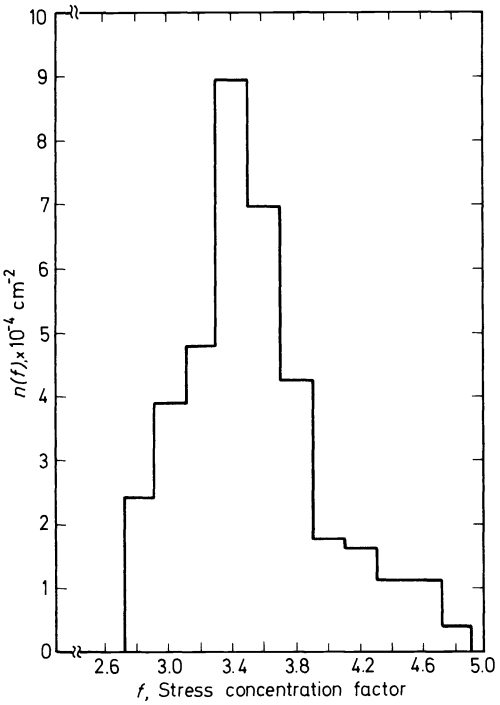

Figure 9. Surface density distribution of sites with different stress concentration factors obtained from traces such as the one shown in *Figure 8*

densities of crazable sites, with increase in the deviatoric shear stress, is of a subtle origin. It will be recalled that the discussion in Section 4 on the mechanical coupling of the porosity inhomogeneity to the elastically strained surroundings led to a requirement, given by equation (15), that the cavitational localization must take place while the local initial porosity $\beta_i < \beta_{crit}$. This requires the presence of a local concentrated negative pressure p_a that must exceed a critical value given by

$$p_a > \tfrac{2}{3} Y \ln \beta_{crit} = \tfrac{2}{3} Y \ln [1/\{1 + (2\mu/Y)\}] \tag{34}$$

for localization to occur. Thus when the stress concentration is too small to elevate the applied negative pressure to the critical level, no localization is possible. Hence, for any given level of applied stress there will be a critical magnitude for a stress concentration factor below which no localization can occur. This critical stress concentration factor will decrease with increasing stress. Therefore with increasing stress an increasing portion of the distribution of the surface stress concentrations becomes potentially available for craze nucleation. As was discussed earlier in connection with *Figure 3*, the required negative pressure for pore expansion decreases somewhat with increasing deviatoric shear stress. Thus, even when the externally applied negative pressure is held constant, an increasing deviatoric shear stress allows

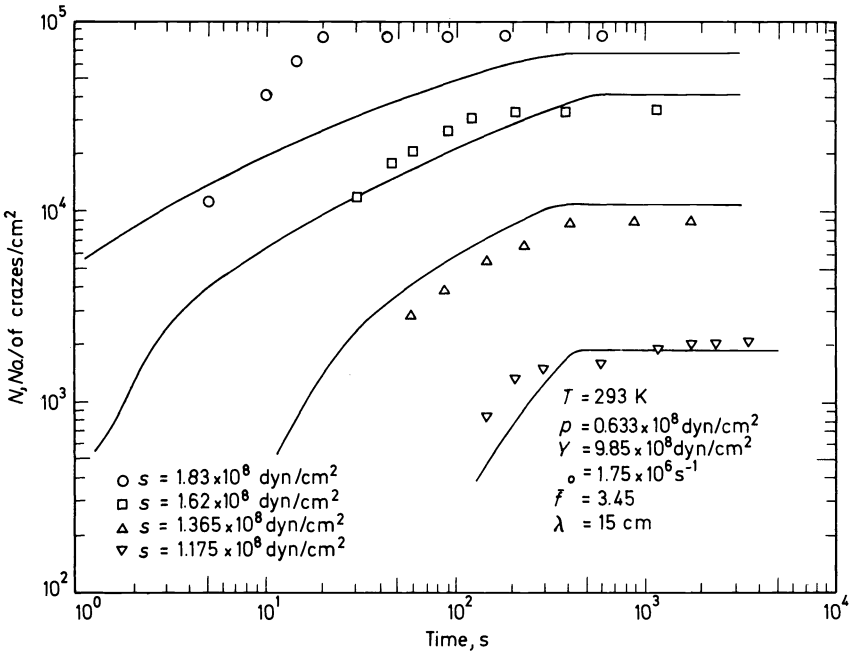

Figure 10. Increase of craze density as a function of time in specimens under different applied deviatoric shear stresses and constant negative pressure, at room temperature. Solid curves on basis of equations (37), (38), (40)

this constant negative pressure to expand an increasing portion of the potential crazable sites of the surface. Hence the increase in the level of asymptotic craze density with increasing deviatoric shear stress under a constant negative pressure. We will now proceed and put this qualitative description on a quantitative basis.

Let $n'(f')$ be the lineal density of grooves with a stress concentration between f' and $f' + \mathrm{d}f'$, as is obtainable directly from a surface topographical scan shown in *Figure 8*. If, as discussed above, there is an additional secondary roughness with a wavelength of λ which tends to amplify the local stress concentrations f' by a constant factor q, then it is possible to define a new areal density of sites $n(f)$ with stress concentration between f and $f + \mathrm{d}f$, given by

$$n(f) = (1/\lambda)n'(f) \tag{35}$$

$$f = qf' \tag{36}$$

Under a given set of normalized applied stresses η and ξ, the cumulative density of surface crazes which will have nucleated after a time t is then given by

$$N(t) = \frac{1}{\lambda}\int_{f(\eta,\xi,t)}^{\infty} n'(f)\,\mathrm{d}f = \int_{f(\eta,\xi,t)}^{\infty} n(f)\,\mathrm{d}f \tag{37}$$

where $f(\eta, \xi, t)$ is obtained by solving equation (28b) for f. This gives

$$f = \frac{\ln \dot{\beta}_0 t}{2\xi} \left\{ \left[1 + \frac{4\xi(A/Y)}{\eta \ln \dot{\beta}_0 t \{1 + \xi^2/3\eta^2\}^{\frac{1}{2}}} \right]^{\frac{1}{2}} - 1 \right\} \tag{38}$$

which is then used as the lower limit of integration in equation (37) and gives the time dependent advance of the operational process front of craze nucleation from right to left on the stress concentration spectrum of *Figure 9*. New craze nucleation will cease when the operational process front arrives at the cut-off stress concentration explained above for which the initial local porosity is just β_{crit} given by equation (15). To find the critical cut-off stress concentration factor, $f_{cut\text{-}off}$, we start with the actual 'locus' for pore expansion under a local set of stresses s and p, given in *Figure 3*, and approximate this by the following expression (for small β):

$$(3p/2Y) \simeq \ln (1/\beta) \{1 - 9(s/Y)^4\}^{\frac{1}{2}} \tag{39}$$

Substituting for $\beta = \beta_{crit}$ and for the local s and p the functional forms given in equations (22a) and (22b), subject to the restriction of equation (27), we obtain a quadratic equation for $f^2_{cut\text{-}off}$ in terms of the externally applied η and ξ. The solution of this quadratic equation gives

$$f^2_{cut\text{-}off} = \frac{-[\xi/\ln\{1 + (2\mu/Y)\}]^2 \pm \sqrt{[[\xi/\ln\{1 + (2\mu/Y)\}]^4 + 36(\xi^2/3 + \eta^2)^2]}}{18(\xi^2/3 + \eta^2)^2} \tag{40}$$

Using equations (37), (38) and (40), it is possible to fit them to the experimental data for four deviatoric shear stresses of *Figure 10*. This requires shifting the centre of gravity of the spectrum of stress concentrations to $\bar{f} = 3.45$, choosing $\dot{\beta}_0 = 1.75 \times 10^6\ s^{-1}$ and $\lambda = 15$ cm. The fit obtained is satisfactory. Some of the discrepancies shown in *Figure 10* are attributable to the unavoidable variation of surface topography between specimens which was detectable from the interference line plots of the type given in *Figure 8* for different specimens.

7. CRAZE NUCLEATION FROM RUBBERY HETEROGENEITIES AND THE PARTICLE SIZE EFFECT OF HIGH IMPACT POLYMERS

It has been found empirically that the incorporation of a certain volume fraction of a rubbery phase in glassy polymers eliminates their brittleness and imparts rather attractive amounts of toughness. The actual mechanism of this increased toughness was established only relatively recently by Bucknall and Smith[42] as being due to the production of a large number of crazes from second-phase particles into which the rubbery phase segregates. In this manner, by a proper choice of the second-phase particle size and spacing, it is possible to fill the volume of the glassy polymer matrix between second-phase particles with a large volume fraction of craze matter and thereby enable the polymer to undergo a dilational mode of plasticity. Experience has shown that

in order to achieve high toughness it is necessary to nucleate and develop as many internal crazes as possible without permitting either these crazes to transform into cracks or the second-phase particles to decohere from the matrix. For this it has been necessary to use a high molecular weight glassy polymer to assure craze matter stability, to graft the rubbery phase to the matrix, and to control the particle shape and size for a given volume fraction of second phase. Many of these details have been thoroughly discussed by Kambour[25], to which reference the reader is referred for additional detail. We wish to concentrate here only on the effect of size of the second-phase particles.

It has been generally appreciated that for a given volume fraction of second phase the toughness reaches a maximum for a particle size in the range of 1–2 μm[43]. There appear to be several contributing reasons for this result. *Figure 11* shows second-phase particles in a microtomed and specially stained section of a rubber modified polystyrene which had been subjected to tension that had produced a large number of crazes between the particles. As can be seen from this figure, the particles themselves are tightly filled with occluded spherical particles of matrix polystyrene for which the rubbery phase appears to act merely as a cement. Hence, the incorporation of a small volume fraction V_r of rubber produces a much larger volume fraction V_p of second-phase particle if the volume fraction V_m of matrix material in the particle is large, i.e.

$$V_p = V_r/(1 - V_m) \tag{41}$$

Experience shows that although there is some variation in the size d_m of occluded matrix particles inside the second-phase particles, there is no clear relationship between the second-phase particle size d and d_m. Thus, while large second-phase particles can contain a great number of tightly packed matrix particles, very small second-phase particles may contain only a few matrix particles or none at all. The stress concentration around such composite particles depends on their effective shear modulus. Bucknall[44] has computed from Goodier's[45] theory the stress concentration on the equatorial regions of spherical particles. Since the special form of the phase distribution shown in *Figure 11* inside the particles produces only a small increase of the effective modulus above that of rubber, which itself is only a small fraction of the glassy polymer, there will be no significant change in the stress concentration from that for a particle filled with rubber alone. Since the initiation of crazes depends on the local deviatoric shear stress s and negative pressure p, and not on any single component of tensile stress, it is necessary to compute these stresses from Goodier's[45] theory. When this is done, we find for the local stresses s and p along the equator of the particle:

$$s = 1.9781\,(T/\sqrt{3}) \tag{42}$$

$$p = 2.1836\,(T/3) \tag{43}$$

where T is the applied tensile stress at a large distance from the particle, and the terms in parentheses give the deviatoric shear stress and negative pressure, respectively, in the distant field. Broutman and Panizza[46] have investigated by a numerical technique the interaction between particles and have shown

that such interactions increase monotonically with increasing volume fraction but become important only when the volume fraction of rubber exceeds ten per cent. Most commercial rubber-modified polymers fall well within this limit for which no such corrections are necessary.

Inspection of *Figure 11* shows that the interphase between the composite second-phase particles and the matrix is rippled, suggesting that additional stress concentrations may have to be considered. Significantly, such ripples

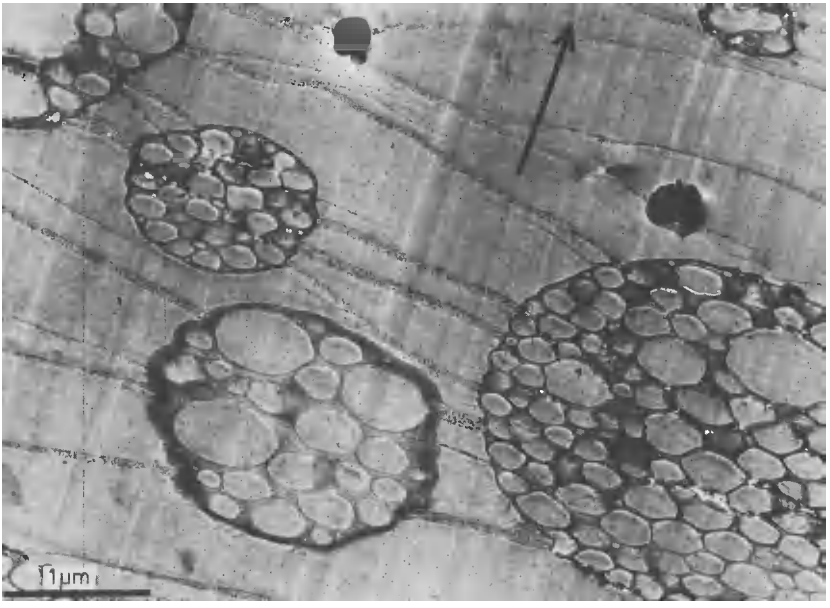

Figure 11. Crazes in rubber modified polystyrene subjected to a plane strain tensile stress in the direction of the arrow. (Photograph courtesy of Dr D. Lee, General Electric Research Laboratory)

dominate along the equatorial areas of the particles. It seems, therefore, that the second-phase particles are very tightly filled with touching particles of occluded matrix and that the distortion expected for soft and homogeneous second-phase particles, due to the extension of the matrix, is actually impeded by a bridge of occluded matrix particles. As is sketched out in *Figure 12*, this can produce an additional interfacial negative pressure by suction along the areas A of rubber pockets. This additional negative pressure can be estimated by considering it a result of a series of interfering indentations produced by the bridging matrix particles of diameter d on the inner surface of the second-phase particle of diameter d_m, giving (for details see Appendix 1)

$$\sigma_{rr_0} = (0.0339)\frac{\pi}{2}T\left\{\left(\frac{T}{\mu}\right)\frac{(d/d_m)^4}{(d/d_m)-1}\right\}^{\frac{1}{2}} \tag{44}$$

From the Hertz theory of indentation stresses (see reference 47) it is readily

calculable that additional principal stresses along the interface will be produced which are

$$\sigma_{rr} = \sigma_{rr_0} \tag{45a}$$

$$\sigma_{\theta\theta} = \sigma_{\psi\psi} = 0.8\sigma_{rr_0} \tag{45b}$$

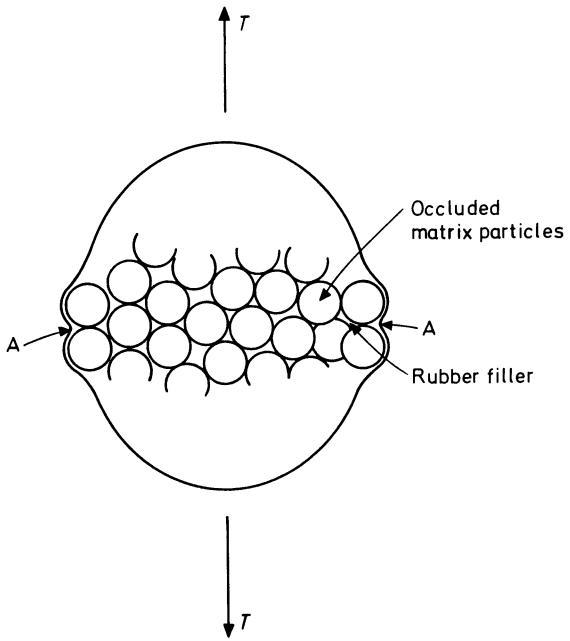

Figure 12. Touching occluded matrix particles inside a composite second-phase particle applying additional stresses on the interface when the matrix is extended

These then combine with the previously computed (equations 42 and 43) stresses s and p to give rise to new net stresses s' and p':

$$s' = 1.9646\,(T/\sqrt{3}) \tag{46}$$

$$p' = 2.5054\,(T/3) \tag{47}$$

Comparison with the magnitudes in equations (42) and (43) shows no change in s' but a significant increase in p'. Based on this, preferential craze nucleation should occur on the interface in the region between two occluded particles. *Figure 11* shows a high incidence of this mode. Thus large composite particles are considerably more effective as craze initiators than small homogeneous particles. For a given volume fraction V_p of second-phase particles, the mean distance between the particles

$$l = d\sqrt{\left(\frac{\pi}{4V_p}\right)} \tag{48}$$

will increase with increasing particle diameter d. Very large crazes are known to convert into cracks when, say, their volume equals a critical value V_c, where the maximum craze opening displacement reaches a critical value b_c. Thus crazes nucleated from large particles of large separation tend to turn into cracks before being re-arrested by other particles, and the polymer tends to be brittle. In this range the strain ε_f to fracture is

$$\varepsilon_f = \varepsilon_c \frac{nV_c}{l^2 d} = \frac{\varepsilon_c}{2} \frac{V_c}{d_s l^2} = \frac{\varepsilon_c}{2}\left(\frac{4}{\pi}\right)\frac{V_c}{d_m d^2} V_p \tag{49}$$

where ε_c is the terminal strain in the crazes and $n = d/d_m$ gives the number of of crazes a particle could nucleate. Here the ductility decreases proportional to the inverse square of the particle size.

When the particle size, and mean particle spacing, decrease, the crazes will be re-arrested by other particles and will not be permitted to convert into cracks prematurely. In this range, then, all crazes bridge across particles and fracture occurs when their opening displacement reaches the critical value b_c. The over-all strain to fracture should then reach its highest value

$$\varepsilon_f = \varepsilon_c n\, 2b_c l^2/l^2 d = \varepsilon_c\, b_c/d_m \tag{50}$$

independent of particle size.

The strain to fracture will decrease again with decreasing particle size when the particles become homogeneous at a size $d \approx d_m$ and lose their craze initiation efficiency. Bucknall[44] has pointed out that another reason for the loss of craze nucleation efficiency of small particles is the shrinking size of the region of enhanced stress to the point where no pores could nucleate in the regions of high stress.

This is a semi-quantitative account of the particle size effect in rubber-modified polymers. Clearly, to formulate a quantitative theory for the optimum particle size, it is necessary to have knowledge of the terminal dimensions of crazes when they convert into cracks. Such information is still lacking.

8. DISCUSSION

Our discussion in the preceding sections has amplified the role of heterogeneities in the crazing of glassy polymers and especially their role as stress concentrators. The importance of stress concentrations in mechanical behaviour of materials has, of course, been recognized for a long time. There are few instances where stress concentrations play so decisive a role as in crazing.

First, it must be recognized that polymers are most remarkable materials. They deform plastically by reaching their ideal shear strength, i.e. their low-temperature yield strength in shear is one-tenth of their shear modulus[40]. Even the strongest of steels falls short from such a performance level by at least a factor of ten. This, however, makes polymers more vulnerable to stress concentrations. Heterogeneities with relatively small differences in mechanical properties and a molecular size level that tend to obstruct inhomogeneous shear could produce enough stress concentration to locally cavitate the material. Homogenizing the material at a molecular level and

finding means for preventing strain softening that tends to make plastic deformation inhomogeneous would suppress premature cavitation and void formation.

Second, stress concentrations at surface grooves or at interfaces of the polymer with particulate inclusions produce local plastic flow that not only initiates such cavitation but also effectively concentrates negative pressure that expands the cavities to form craze nuclei. Absence of such stress concentrations would bring the polymer homogeneously to yield and the insufficient negative pressure in the homogeneous stress field would prevent craze nucleus formation before molecular alignment altogether suppresses crazing. These same processes are, of course, active in the very same sense in rubber-modified polymers.

Heterogeneities in polymers are, naturally, not always detrimental. They can often be used to compensate adverse effects of other heterogeneities. For example, the second-phase particles in rubber modified polymers, discussed in Section 7 above, do not only initiate crazes but they also arrest them. Alternatively, bands of inhomogeneous shear which can form microcracks in a manner discussed in Section 4 or in a more macroscopic manner by impingement on another band[48] can also act as effective craze arresters[49]. In fact, often it becomes possible to obtain toughness with very small rubber particles by initiating shear bands from these particles which have become too small to be effective craze initiators provided the polymer is of a type that undergoes strain softening so that deformation tends to localize into shear bands. These shear bands then interact with and stop the growth of crazes[49, 50].

Although much of the behaviour which we have discussed can be qualitatively and semi-quantitatively understood, fully quantitative description of phenomena requires a much higher level of understanding of molecular-level deformation processes involving strain softening and strain hardening as well as the morphology and stability of craze matter.

ACKNOWLEDGEMENT

I am indebted to Professor J. N. Sultan for pointing out a number of publications in this area which had escaped my attention. This work has been supported by the National Science Foundation under a Grant GH-40467.

REFERENCES

[1] A. Keller and D. P. Pope, *J. Materials Sci.* **6**, 453 (1971).
[2] A. J. Owen and I. M. Ward *J. Materials Sci.* **6** 485 (1971).
[3] R. J. Young and P. B. Bowden, *J. Materials Sci.* **8**, 1177 (1973).
[4] A. Peterlin in E. Baer and V. Radcliffe (eds.) *Polymeric Materials, Relationships Between Structure and Mechanical Behavior*, p. 175. ASM: Metals Park, Ohio (1975).
[5] G. S. Y. Yeh, *J. Macromol. Sci.* **B6** (3), 451 (1972).
[6] G. S. Y. Yeh, *J. Macromol. Sci.* **B6** (3), 465 (1972).
[7] G. S. Y. Yeh and P. H. Geil, *J. Macromol. Sci.* **B1** (2), 235 (1967).
[8] B. Vollmert, this volume, p 183.
[9] P. J. Flory, *Principles of Polymer Chemistry*. Cornell University Press: Ithaca, New York (1953).
[10] R. G. Kirste, to be published (1975).

[11] D. J. Meier, in J. J. Burke and V. Weiss (eds.), *Block and Graft Copolymers*, p 105. Syracuse University Press: Syracuse, New York (1973).
[12] E. Helfand, in L. H. Sperling (ed.), *Recent Advances in Polymer Blends, Grafts, and Blocks*. p 141. Plenum Press: New York (1974).
[13] H. Kawai, T. Soen, T. Inoue, T. Ono and T. Uchida, *Mem. Fac. Engineering Kyoto University*, 33 (Part 4), 383 (1971).
[14] M. J. Folkes and A. Keller, in R. N. Haward (ed.), *The Physics of Glassy Polymers*. p 548. Halsted Press: New York (1973).
[15] P. K. Mallick and L. J. Broutman, *Materials Science and Engineering* (in press).
[16] A. S. Argon, in H. Herman (ed.), *Treatise on Materials Science and Technology*, Vol. 1, p 79. Academic Press: New York (1972).
[17] A. S. Argon, in L. Broutman (ed.), *Composite Materials*, Vol. 5, p 153. Academic Press: New York (1974).
[18] A. Kelly, *Strong Solids*. Clarendon Press: Oxford (1966).
[19] J. C. Halpin and J. L. Kardos, *J. Appl. Phys.* **43**, 2235 (1972).
[20] S. L. Aggarwal, R. A. Livigni, L. F. Marker and T. J. Dudek, in J. J. Burke and V. Weiss (eds.), *Block and Graft Copolymers*, p 157. Syracuse University Press: Syracuse, New York (1973).
[21] B. D. Agarwal and L. J. Broutman, *Fibre Science and Technology*, **7**, 63 (1974).
[22] D. G. Fesko and N. W. Tschoegl, *J. Polymer Sci.* Part C, **35**, 51 (1971).
[23] A. S. Argon, in E. Baer and V. Radcliffe (eds.), *Polymeric Materials, Relationships Between Structure and Mechanical Behavior*, p 411. ASM: Metals Park, Ohio (1975).
[24] S. Rabinowitz and P. Beardmore, in E. Baer, P. Geil and L. Koenig (eds.), *CRC Critical Reviews in Macromolecular Science*, Vol. 1, p 1. CRC Press: Cleveland, Ohio (1972).
[25] R. P. Kambour, *J. Polymer Sci.: Macromolecular Reviews*, **7**, 1 (1973).
[26] A. S. Argon, *J. Macromol. Sci.-Phys.* **B8** (3–4), 573 (1973).
[27] S. N. Zhurkov, V. S. Kuksenko and A. I. Slutsker, in P. Pratt *et al.* (eds.), *Fracture*, p 531. Chapman and Hall: London (1969).
[28] S. N. Zhurkov, V. I. Vettegren, V. E. Korsukov and I. I. Novak, in P. Pratt *et al.* (eds.), *Fracture*, p 545. Chapman and Hall: London (1969).
[29] E. Baer and S. T. Wellinghoff, in *Yield, Deformation and Fracture of Polymers* (outlines of lecture presentations at the 2nd International Conference bearing the same title, at Churchill College, Cambridge, 1973), quoted with the permission of the authors.
[30] A. Thierry, R. J. Oxborough and P. B. Bowden, *Phil. Mag.* **30**, 527 (1974).
[31] A. N. Stroh, *Proc. Roy. Soc. (London)*, **A223**, 404 (1954).
[32] L. E. Nielsen, private communication (1974).
[33] J. R. Rice and D. M. Tracy, *J. Mech. Phys. Solids*, **17**, 201 (1969).
[34] F. A. McClintock and I. F. Stowers, 'User's manual for numerical calculation of plane plastic flow fields by superposing dislocation dipoles', Research Memorandum No. 159 (Fatigue and Plasticity Laboratory, M. E. Dept., MIT, Cambridge, Mass.) (1970).
[35] S. S. Sternstein and L. Ongchin, *Polymer Preprints*, **10**(2), 117 (1969).
[36] G. P. Marshall, L. E. Culver and J. G. Williams, *Proc. Roy. Soc.* (*London*), **A319**, 165 (1970).
[37] A. S. Argon and M. Salama (to be published).
[38] T. S. Wang, M. Matsuo and T. K. Kwei *J. Appl. Phys.* **42**, 4188 (1971).
[39] R. J. Oxborough and P. B. Bowden *Phil. Mag.* **28**, 547 (1973).
[40] A. S. Argon *Phil. Mag.* **28**, 839 (1973).
[41] A. S. Argon and J. Hannoosh (to be published).
[42] C. B. Bucknall and R. R. Smith, *Polymer*, **6**, 437 (1965).
[43] J. D. Moore, *Polymer*, **12**, 478 (1971).
[44] C. B. Bucknall, *J. Materials*, **4**, 214 (1969).
[45] J. N. Goodier, *Trans. Amer. Soc. Mech. Engrs* **55**, 39 (1933).
[46] L. J. Broutman and G. Panizza, *Intern. J. Polymeric Mater.* **1**, 95 (1971).
[47] S. Timoshenko and J. N. Goodier, *Theory of Elasticity*, McGraw-Hill: New York (1951).
[48] D. Hull, in E. Baer and V. Radcliffe (eds.), *Polymeric Materials, Relationships Between Structure and Mechanical Behavior*, p 487. ASM: Metals Park, Ohio (1975).
[49] F. J. McGarry, *Proc. Roy. Soc.* (*London*), **A319**, 59 (1970).
[50] C. B. Bucknall, D. Clayton and W. E. Keast, *J. Materials Sci.* **7**, 1443 (1972).

APPENDIX 1

Development of secondary stresses on interfaces of composite second-phase particles

The radial displacements along the interface of a soft spherical inclusion, of radius a in a stiff, elastic matrix of infinite extent, subjected to a tensile stress T at a large distance from the inclusion is, according to Goodier[45],

$$u_r = -\frac{A}{r^2} - \frac{3B}{r^4} + \left[\left(\frac{5-4\nu_1}{1-2\nu_1}\right)\frac{C}{r^2} - 9\frac{B}{r^4}\right]\cos 2\theta \qquad \text{(A.1)}$$

where

$$A \simeq -\frac{Ta^3}{8\mu_1}\left(\frac{6-5\nu_1}{7-5\nu_1}\right) \qquad \text{(A.2a)}$$

$$B \simeq \frac{Ta^5}{8\mu_1}\frac{1}{(7-5\nu_1)} \qquad \text{(A.2b)}; \qquad C \simeq \frac{Ta^3}{8\mu_1}\frac{5(1-2\nu_1)}{(7-5\nu_1)} \qquad \text{(A.2c)}$$

where θ is the spherical altitude angle measured from the tensile direction; μ_1 and ν_1 are the shear modulus and Poisson's ratio for the matrix material; and the constants A, B, and C are evaluated for a very soft inclusion for which $\mu_2 \ll \mu_1$.

It can be shown from Goodier's solution that the average radial interfacial traction on the soft, homogeneous inclusion is of a smaller order than the two tangential stresses on the side of the matrix at $\theta = \pi/2$.

If the occluded matrix particles inside the composite particle are tightly enough packed to form a bridge across the heterogeneity, then the radial displacements in equation (A.1) will be prevented by local indentations as sketched in *Figure 12*. Such indentations then produce additional radial tractions which can be computed from the Hertz theory of contact between two spherical objects[47].

The indentation α of an internal spherical surface of radius $d/2$ by a smaller sphere of radius $d_m/2$ is, from this theory,

$$\alpha = 1.23\,((2P^2/E^2)\,(d - d_m)/dd_m)^{\frac{1}{3}} \qquad \text{(A.3)}$$

Equating α to u_r we find the indentation force P

$$P = (0.0339)\mu_1\left(\frac{d}{2}\right)^2\left\{\left(\frac{T}{\mu_1}\right)^3\frac{1}{[(d/d_m)-1]}\right\}^{\frac{1}{3}} \qquad \text{(A.4)}$$

where the constants A, B, C were evaluated for $\nu_1 = 0.3$ and substituted into equation (A.1), setting $\theta = \pi/2$, $r = d/2$.

Considering the indentation forces to be distributed as a sinusoidally varying traction of a wavelength d_m and having compensating regions of negative pressure so as not to violate the condition of negligible average radial traction, one computes the peak local radial traction σ_{rr_0} to be

$$\sigma_{rr_0} = T\frac{(0.0339)\pi}{2}\left\{\left(\frac{T}{\mu_1}\right)\frac{(d/d_m)^4}{(d/d_m - 1)}\right\}^{\frac{1}{3}} \qquad \text{(A.5)}$$

which is the form given in equation (44) of the text.